Limnol. Oceanogr., 59(5), 2014, 1715–1732

doi:10.4319/lo.2014.59.5.1715

Surface biological, chemical, and optical properties of the Patagonian Shelf coccolithophore bloom, the brightest waters of the Great Calcite Belt

W. M. Balch,[1,*] D. T. Drapeau,[1] B. C. Bowler,[1] E. R. Lyczkowski,[1] L. C. Lubelczyk,[1] S. C. Painter,[2] and A. J. Poulton [2]

[1] Bigelow Laboratory for Ocean Sciences, East Boothbay, Maine
[2] National Oceanography Centre, University of Southampton, Waterfront Campus, Southampton, United Kingdom

Abstract

We report surface observations of a mesoscale coccolithophore bloom at the shelf break of the Patagonian Shelf during December 2008, representing the densest coccolithophore population in the Southern Ocean. The bloom was most intense within the Falklands Current, northeast of the Falkland Islands. *Emiliania huxleyi* dominated bloom waters, with a mixed *E. huxleyi* and *Prorocentrum* sp. dinoflagellate bloom to the west and mixed assemblage of diatoms, dinoflagellates, and flagellates to the east. Optical measurements of coccolith light scattering, analytical measurements of their calcite, and microscopic counts all showed this to be an intense coccolithophore bloom. Average particulate inorganic carbon per coccolith in the bloom was low, typical of the B coccolith morphotype and in agreement with independent measurements made by scanning electron microscopy. Highest particulate inorganic carbon (measured optically and chemically) was observed when residual nitrate (defined as the difference, $[NO_3^-] - [Si(OH)_4]$) was 10–17 μmol L^{-1} and nitrate to phosphate ratios were close to Redfield values. Elevated particle backscattering was observed in the *E. huxleyi* bloom, whereas the highest particle scattering occurred in the adjoining *Prorocentrum* sp. bloom. Backscattering from coccolithophores represented up to 50% of the total backscattering (from organic and inorganic particles) along the main axis of the *E. huxleyi* bloom. Chlorophyll-specific absorption in the coccolithophore bloom was typical of marine phytoplankton. Residual nitrate plotted vs. temperature showed that the *E. huxleyi* bloom was associated with waters between 5°C and 15°C, with depleted silicate. Results suggest that previous drawdown of silicate by diatoms occurred prior to the densest *E. huxleyi* blooms over the Patagonian Shelf. We speculate that such conditions might also be important for annual development of the broader Great Calcite Belt and other coccolithophore blooms.

Coccolithophores are unicellular calcium carbonate ($CaCO_3$)-producing phytoplankton (class Prymnesiophyceae, family Haptophyceae) that significantly influence the partitioning of the various components of dissolved inorganic carbon (DIC) and affect global biogeochemical cycles. There is a strong correlation between sinking organic carbon and $CaCO_3$, suggesting that $CaCO_3$ acts as ballast for much of the export production of organic carbon to the deep sea (Francois et al. 2002). Blooms of the cosmopolitan coccolithophore *Emiliania huxleyi* have been studied mostly in the northern hemisphere (Holligan et al. 1993). However, coccolithophore blooms, as observed from space, are found globally, mostly in the higher latitude waters of both hemispheres (Brown and Yoder 1994) and are mostly formed by the species *E. huxleyi*.

Even within the ubiquitous species *E. huxleyi*, conditions selecting for coccolithophore blooms are unclear. Factors that often determine the prevalence of coccolithophorid blooms vs. blooms of other marine phytoplankton are (1) water column stability, (2) high incident irradiance, and (3) relatively low nutrient concentrations (Iglesias-Rodriguez et al. 2002; except we will show below that this not true in the Patagonian Shelf region). Phosphate limitation has been hypothesized to be a critical factor promoting blooms (Paasche and Brubak 1994), based on physiological studies indicating that *E. huxleyi* has an exceptionally high affinity for orthophosphate and may be able to utilize organic phosphorus using extracellular phosphatases (Satoh et al. 2009). However, observations from Pacific blooms (eastern Bering Sea 1997–2000) led to a complete revision of the relationships between nutrient availability and bloom formation (Tyrrell and Taylor 1995). *E. huxleyi* blooms are usually associated with moderate stratification and occur within a few weeks of the summer solstice in each respective hemisphere (Balch 2004).

The advent of the particulate inorganic carbon (PIC) remote sensing algorithm allowed quantitative estimates of coccolithophore PIC concentrations in bloom and non-bloom waters alike (Balch et al. 2005), and global PIC time series have resulted. Using remote sensing, it can be seen that elevated PIC concentrations are disproportionately more frequent in the southern hemisphere, particularly during austral summer. Indeed, 68% of the global PIC standing stock falls south of the equator, and 26% of global suspended PIC is found between 40°S and 60°S (Balch et al. 2005).

The Great Calcite Belt—A consistent southern hemisphere feature in PIC imagery has been the presence of a massive belt of elevated PIC concentrations near the subtropical, Subantarctic Front and Polar Front, around the Southern Ocean. This large band of water with elevated PIC (referred to as the "Great Calcite Belt" or hereafter as the GCB; Balch et al. 2011*a*) has been observed in all

* Corresponding author: bbalch@bigelow.org

National Aeronautics and Space Administration (NASA) ocean-color missions since 1978, with minor variations (Coastal Zone Color Scanner, Sea-viewing Wide Field-of-view Sensor [SeaWiFS], Moderate Resolution Imaging Spectroradiometer [MODIS], and Visible Infrared Imaging Radiometer Suite missions; http://oceancolor.gsfc.nasa.gov/; but note that there was no ocean-color remote sensing for 11 of those years, 1986–1997). The GCB appears at $\sim 40^{\circ}$S and extends southward to $\sim 60^{\circ}$S with an area of $\sim 56 \times 10^6$ km^2, 16% of the global ocean (Balch et al. 2011*a*). PIC concentrations appear to be highest just east of the Drake Passage, over the Patagonian Shelf; and PIC concentrations gradually diminish to the east, with significant concentrations through the Indian and Pacific sectors of the Southern Ocean. The GCB may be the largest elevated reflectance region, characterized by increased abundance of Haptophyte algae (coccolithophores). Note that the concentrations of PIC in the GCB are not uniformly high, as seen in mesoscale coccolithophore blooms (10–20 μmol C L^{-1}; Holligan et al. 1993). Instead, PIC concentrations are $\sim 10\times$ less in the GCB, 0.7–2 μmol C L^{-1}. Such concentrations in the GCB are still 15–40$\times$ higher than the lowest PIC concentrations seen in the world ocean (0.05 μmol PIC L^{-1}; Balch et al. 2005).

The GCB has been sampled from ships throughout the Southern Ocean, and studies have confirmed the presence of *E. huxleyi* using microscopy and coccolith optical properties. Bright *E. huxleyi* coccolithophore blooms have been sampled previously over the Patagonian Shelf region (Garcia et al. 2008; Painter et al. 2010; Garcia et al. 2011). Multiple reports back to the 1960s show that *E. huxleyi* is found in all four sectors of the Southern Ocean (*see* Holligan et al. 2010 and references therein). Backscattering of coccolithophores also indicates their presence in the Southern Ocean (Balch and Utgoff 2009; Balch et al. 2011*a*), and systematic observations across the entire Atlantic and Indian sectors of the Southern Ocean show that coccolithophores are most abundant at the major frontal boundaries (W. Balch, P. Lam, B. Twining, N. Bates and H. Smith unpubl.). Winter et al. (2013) suggest that this species is spreading poleward with climate change.

Oceanographic context—The Patagonian Shelf lies offshore of the Argentinean and Uruguayan coasts with a well-defined shelf slope break following the 200 m isobath from 35°S to 55°S. South of the Patagonian Shelf are the Drake Passage and the Southern Ocean, both high-nutrient, low-chlorophyll (HNLC) areas in which macronutrients are abundant and iron is scarce (Boyd et al. 1999). This relatively unexplored region is one of the world's largest and most productive shelf regions where bright coccolithophore features are seen in satellite data (Signorini et al. 2006). The southward-flowing Brazil Current is warm and saline, whereas the northward-flowing Falklands Current (FC) carries cool, less saline, nutrient-rich subantarctic water toward the equator. The two currents mix at a confluence zone whose characteristics and dynamics are poorly understood (Garzoli et al. 1992).

Satellite images show that the Patagonian Shelf is characterized by a band of high chlorophyll associated with dense phytoplankton blooms and long (several hundred kilometers) streaks of highly reflective water parallel to the shelf break (Romero et al. 2006). The uniqueness of this region lies in (1) the recurrent optical patterns seen over years of satellite ocean-color imagery showing one or two well-defined, high-reflectance streaks along the shelf break (Romero et al. 2006; *see* also http://www.noc.soton.ac.uk/soes/staff/tt/eh/pat.html); (2) in situ taxonomic data showing *E. huxleyi* as a regular part of the phytoplankton community; and (3) the fact that the Patagonian Shelf represents a significant sink for atmospheric CO_2 (Bianchi et al. 2005), although the presence of coccolithophore blooms may complicate this interpretation because calcification in such blooms can increase the PCO_2 by as much as 5.07 μPa (Holligan et al. 1993).

The purpose of the expedition, Coccolithophores of the Patagonian Shelf 2008 (COPAS'08), was to systematically document the intense coccolithophore bloom of the Patagonian Shelf, the highest reflectance region within the GCB (as seen by satellite). Specifically, our goal was to determine where the center of the feature was located, its bio-optical, nutrient, hydrographic, and ecological characteristics and, ultimately, to elucidate the factors affecting its formation. The first paper from this work described the oceanographic conditions and basic nutrient distributions associated with this feature (Painter et al. 2010). The second paper described the biometric properties of the *E. huxleyi* populations and how these related to the nutrient and carbonate chemistry (Poulton et al. 2011). A third paper (Poulton et al. 2013) described the calcite production and general characteristics of the Patagonian Shelf bloom in terms of its ecology, biogeochemistry and cellular calcification rates relative to other coccolithophore blooms in the world ocean. Here, we describe the surface properties of the bloom in terms of chlorophyll *a* (Chl *a*), PIC, detached coccolith and coccolithophore concentrations, nutrient dynamics, and bio-optical properties. We focus mostly on the surface description of the bloom, as perceived by satellite remote sensing and ship measurements.

Methods

This work was carried out during the COPAS'08 cruise of the R/V *Revelle* (cruise "Knox 22RR"), which sailed from Montevideo, Uruguay, on 4 December 2008 and arrived in Punta Arenas, Chile, on 03 January 2009. The cruise track (Fig. 1) consisted of several legs or "lines" either across or parallel to the shelf break bloom(s). Line A transited southwest from Uruguay, through waters heavily influenced by the Rio de la Plata, across the shelf break into the warm, saline Brazil Current. This was followed by the longest transit line (B) to the southwest, crossing obliquely back across the shelf break, onto the Argentine shelf. Next, a series of east–west survey legs were performed, targeting the shelf-break region north and south of the Falkland Islands (FIs), where previous ocean-color satellite imagery suggested the presence of bright coccolithophore blooms. These east–west survey legs were continued across the shelf, then radially across the shelf, around the FIs (legs C-A2;

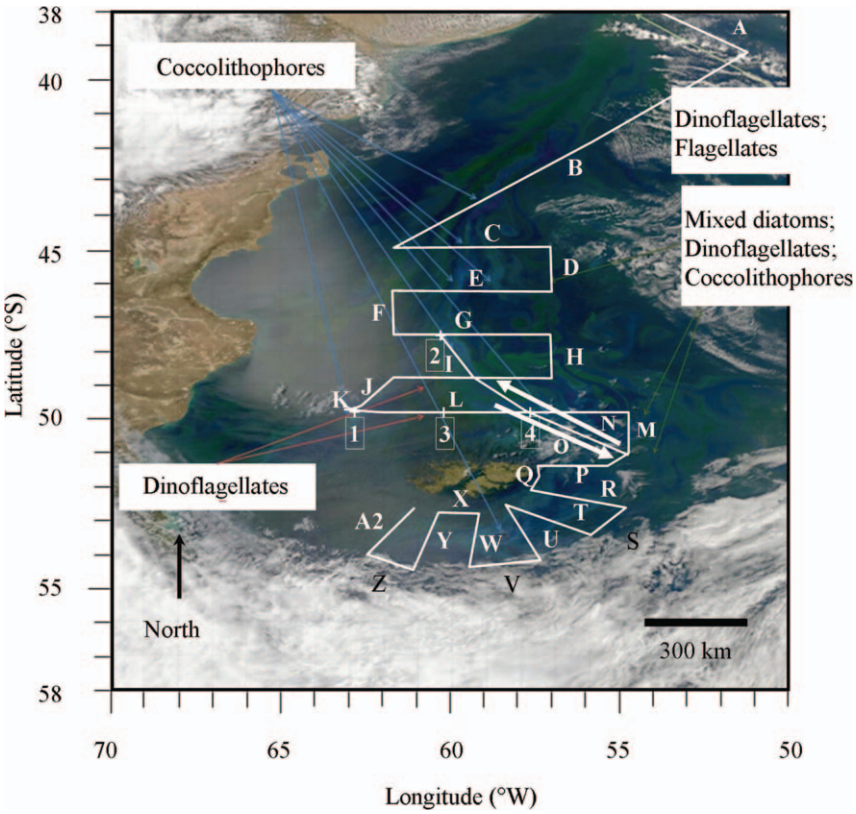

Fig. 1. NASA MODIS Aqua true-color image of the southwest Atlantic off of Argentina and the Falkland Islands (10 December 2008; image processed by Norman Kuring, NASA, Goddard Space Flight Center). Qualitative observations of the dominant phytoplankton functional groups are noted (based on preparations using the filter-freeze transfer technique (Hewes and Holm-Hansen 1983), shipboard light microscopy (epifluorescence [to visualize chlorophyll and phycoerythrin fluorescence], polarized [to observe birefringent coccoliths and coccospheres], and bright field), and FlowCAM. The ship's cruise track is shown as a black line. Letters next to each section of cruise track designate different "lines" of the cruise. Arrows show direction of travel for two identical lines, N and O, sampled in opposite directions. Coccolithophores dominated in the cyan-colored waters (Painter et al. 2010; Poulton et al. 2011). A smaller and less concentrated coccolithophore bloom was observed on the western end of line L. The dinoflagellate population north of the Falklands had high chlorophyll concentrations and contained *Prorocentrum* sp. On the eastern side of the coccolithophore bloom was a mixed population of diatoms, dinoflagellates, and coccolithophores.

Fig. 1). The only exception to this radiator sampling pattern were legs O and N, which went through the main axis of the coccolithophore bloom, along the major axis of the FC (line O), then a reciprocal course to the southeast, against the main axis of the FC (line P).

The station plan had measurements of conductivity, temperature, and depth (CTD) at ~ 44 km horizontal resolution for line A from Montevideo. For line B, water sampling was performed at every station, each separated by 115 km. For all subsequent legs, CTD stations were ~ 30 km apart and every other station was processed for a vertical water cast and CTD profile. This station plan translated to a total of 152 stations (some with multiple CTD casts, for a total of 168 CTD casts), with 76 stations with both full-CTD and water casts).

On casts where water was taken, samples were drawn from Niskin bottles in the following order: oxygen, carbonate chemistry (DIC and alkalinity), nutrients, primary productivity (and calcification), particulates, Chl *a*, cell counts, particle image analysis (FlowCAM®), and salinity. Sampling was carried out at the following fixed light depths relative to surface irradiance: 50, 30, 20, 10, 5, 3, 1, and 0.1%. These depths were calculated based on one of two methods: (a) during daylight hours (10:00 h–14:00 h local time), percentages of surface irradiance were derived from the downcast photosynthetically available radiation (PAR) profile immediately preceding bottle firing or (b) at all other times, light depths were based on the previously determined relationship between beam transmittance and diffuse attenuation of PAR (Balch et al. 2011*b*).

Water samples were taken at the abovementioned eight light depths per station for the following: particulate organic carbon (POC) and particulate organic nitrogen (PON; Joint Global Ocean Flux Study [JGOFS] 1996), PIC ($CaCO_3$; Poulton et al. 2006), biogenic silica (Brzezinski and Nelson 1989), coccolithophore counts (processed using

the Canada Balsam technique for enumeration of calcite particles; Balch et al. 2011*a*), fluorometric Chl *a* measurements (surface bottles always run in triplicate; JGOFS 1996), and FlowCAM samples (for enumeration and identification of microplankton, 20–200 μm, and nanoplankton, 5–20 μm; Poulton and Martin 2010). Positive identification of the smallest particles (5–10 μm) to the class level was difficult due to the limited optical resolution.

The bio-optical underway system was run continuously over the course of the trip. This system, described elsewhere (Balch et al. 2008), is run by Labview software and measures temperature, salinity, Chl *a* fluorescence, and backscattering at 531 nm (using a Western Environmental Technology Laboratories [WET Labs] ECO-VSF® sensor). At a period of every 3–4 min, 10% glacial acetic acid is injected into the flow stream, upstream of the ECO-VSF, to reduce the seawater pH to 5.4–5.5, below the dissociation point for calcite. In short, a pH sensor downstream of the sample chamber measures the pH, and this information is used by the Labview software to regulate the acid controller. Once 60 s (or whatever is required for a statistically significant measurement) of data were collected at ambient pH, the acid controller injects glacial acetic acid (0.2 μm filtered) into the seawater stream, passing through a mixing coil to thoroughly mix it with the seawater stream. Once the pH downstream of the ECO-VSF drops to a pH of 5.4, the backscattering is remeasured for 60 s. The difference in backscattering between raw and acidified streams represents acid-labile backscattering, which can be directly related to the concentration of suspended PIC using a PIC backscattering cross-section of $\sim$ 1.5–4 m^2 $(mol\ PIC)^{-1}$ (Balch et al. 1999).

The flow-through system had a separate loop that passed through a WET Labs nine-wavelength absorption and attenuation meter (ac-9). In the flow path to the ac-9 was a solenoid valve that periodically diverted the seawater stream serially through a 1 μm filter, then a 0.2 μm filter, prior to running the water through the ac-9. Every 2 min, the solenoid would alternate between raw and filtered (0.2 μm) seawater, providing absorption and attenuation at nine spectral wavelengths across the visible spectrum, thus providing the absorption and attenuation of total suspended particulate plus dissolved material, just dissolved material, and (by difference) particulate matter.

Results

Remote sensing—Satellite-derived true-color imagery showed a band of high-reflectance, turquoise-colored water within the FC, with bands of green, high-chlorophyll water over the shelf and further east (Fig. 1). Differences in algal community composition were apparent, based on qualitative shipboard microscopy (as indicated in Fig. 1) plus FlowCAM analysis. Sea surface temperature (SST) results from the MODIS Aqua daytime SST product (11 μm band) for December 2008 (Fig. 2A) showed the presence of warm, Brazil Current water reaching south into the northeast region of the survey area, across the offshore end of survey line A. Cooler FC water was found in the survey region south and east of the FIs, with cool temperatures extending along the Patagonian Shelf break further to the north, with a tongue of 14–16°C water reaching northeastward across survey line A, inshore of the warm tongue of Brazil Current water. Satellite-derived PIC concentrations showed the presence of a band of PIC-rich water extending from south of the FIs, around the east side of the islands, and extending toward the northwest, following the shelf break (Fig. 2B). Highest PIC concentrations were generally seen at temperatures from 7°C to 9°C (*see* isopleths of temperature overlaid on Fig. 2B). Highest PIC concentrations were seen in waters with salinities of 33.75 to 34.25 (Fig. 2C) and density anomalies (sigma–theta) $>$ 26 (Fig. 2D). Underway surface density measurements showed the influence of high-density water from south of the subantarctic front (sigma–theta of 26–27) that flowed in a counterclockwise fashion around the FIs, staying at the shelf break further north. Strong horizontal density gradients were observed at the confluence of the Falklands and Brazil Currents ($\sim$ 40°S).

Distribution of phytoplankton biomass—Discrete Chl *a* samples (an indicator of phytoplankton biomass) taken from the top 10 m of the water column showed typical concentrations of $\sim$ 1 $\mu g\ L^{-1}$, with a range of $\sim$ 0.1 $\mu g\ L^{-1}$ to 2 $\mu g\ L^{-1}$ (Fig. 3A). Lowest Chl *a* concentrations of the cruise ($< 0.1\ \mu g\ L^{-1}$) were observed at the southeast end of line A and the northeast end of line B, in waters of the southward-flowing Brazil Current (Painter et al. 2010). Low Chl *a* concentrations were also observed at the west end of Line L, as well as at 57.65°W (Fig. 3A). These discrete chlorophyll data were used to calibrate the underway fluorescence data to units of $\mu g\ L^{-1}$ (Fig. 3B). These higher resolution data showed a region of low Chl *a* water ($< 0.5\ \mu g\ L^{-1}$) in the FC flowing counterclockwise around the FIs, with other low patches extending along the Patagonian Shelf break. MODIS Aqua ocean-color imagery (collection 6; Level 3; 9 km–binned, monthly averaged data; Fig. 3C) showed the same band of low Chl *a* concentration around the FIs (albeit a bit higher in concentration than was actually measured), extending as a narrow band just offshore of the Shelf Break (Fig. 1). Inshore of this low Chl *a* water was water over the shelf with elevated Chl *a*, extending from just north of the FIs all the way north to the region off the Rio de la Plata. The region of low Chl *a* water was similar within these three different chlorophyll data sets (discrete, continuous, and satellite-derived).

Coccolithophore distribution—The biomass of coccolithophores and associated PIC was described using a number of different techniques, including satellite remote-sensing PIC measurements (Fig. 2B), inductively-coupled plasma optical emission spectroscopy (ICP–OES), microscopy, and bio-optical measurements (Fig. 4). ICP–OES measurements of particulate calcium (converted to PIC equivalents) showed that the peak PIC concentration was observed on Line L (Fig. 4a, *see* also Fig. 1), with concentrations $> 4\ \mu mol\ C\ L^{-1}$ situated in waters < 9°C, wrapping around the FIs (Fig. 4A), similar to that observed in the MODIS-Aqua satellite PIC image

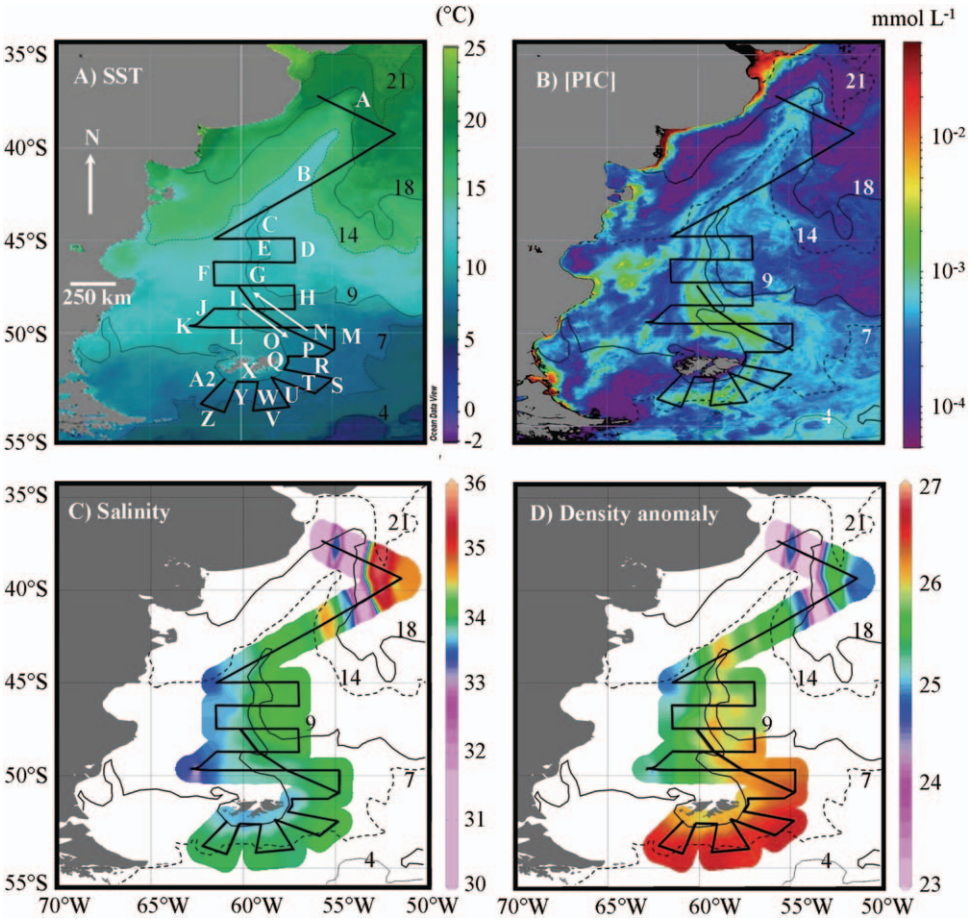

Fig. 2. Satellite-derived sea surface temperature (SST), PIC, and ship-derived hydrographic measurements. (A) MODIS Aqua daytime SST (11 μm band; °C) averaged over December 2008. Isopleths of temperature noted. (B) MODIS Aqua image of PIC concentration (mol PIC m^{-3}) for same time period as in panel A. (C) Shipboard surface salinity made with underway system. (D) Surface water density anomaly (sigma–theta). Cruise track is overlaid on all four panels along with contours of the SST for reference. Diagonal line through radiator pattern was run through the long axis of the high-density coccolithophore bloom. Each line of the cruise track is designated with a white uppercase letter. Arrows show direction of travel for identical lines, M and O.

(Fig. 2B). Results of the microscope counts of detached coccoliths showed similar patterns (Fig. 4B), with peak concentrations of $>$ 250,000 coccoliths per milliliter northeast of the FIs. A separate, less intense bloom was seen northwest of the FIs, at the western end of line L, characterized by PIC concentrations of $\sim$ 1 μmol C L^{-1} and 150,000 detached coccoliths per milliliter (Fig. 4A,B, respectively). Moderately high concentrations of coccoliths and coccolithophores were seen along lines C and G (Fig. 4A,B). Maximum concentrations of plated coccolithophore cells were $\sim$ 1000 cells mL^{-1} (Fig. 4C) in the FC, in waters between 7°C and 9°C with covariance between the coccolithophore cells and coccolith concentration (Fig. 4B,C). The ratio of detached coccoliths to plated cells reached 350 northeast of the FIs, along line L (Fig. 4D). Continuously derived shipboard optical measurements of acid-labile backscattering (b'_b) showed highest values in regions of abundant PIC and coccolithophores (Fig. 4E). Shipboard measurements of b'_b showed a similar pattern, with the most elevated b'_b being northwest and northeast of the FIs, respectively, in waters of 7°C to 9°C. A narrow band of elevated b'_b water originating south of the FIs wrapped around the eastern part of the FIs and then toward the northwest along the shelf break. Elevated shipboard b'_b values could be observed as far north as 42.5°S. Values of b'_b reached as high as 50% of the total particle backscattering in the major axis of the FC, especially in the intense bloom along 50°S (along line L; Fig. 4F). Without exception, the warmest subtropical waters associated with the Brazil Current (east end of line A and northeast end of line B) were characterized by low PIC, low coccolith concentrations, low coccolithophore concentrations, and low b'_b.

Nutrients and residual nitrate—Nitrate measurements confirmed that the surface waters of the FC between temperatures of 7°C and 9°C had typical concentrations of 15 μmol L^{-1} (Fig. 5A). Surface ammonium showed patchy

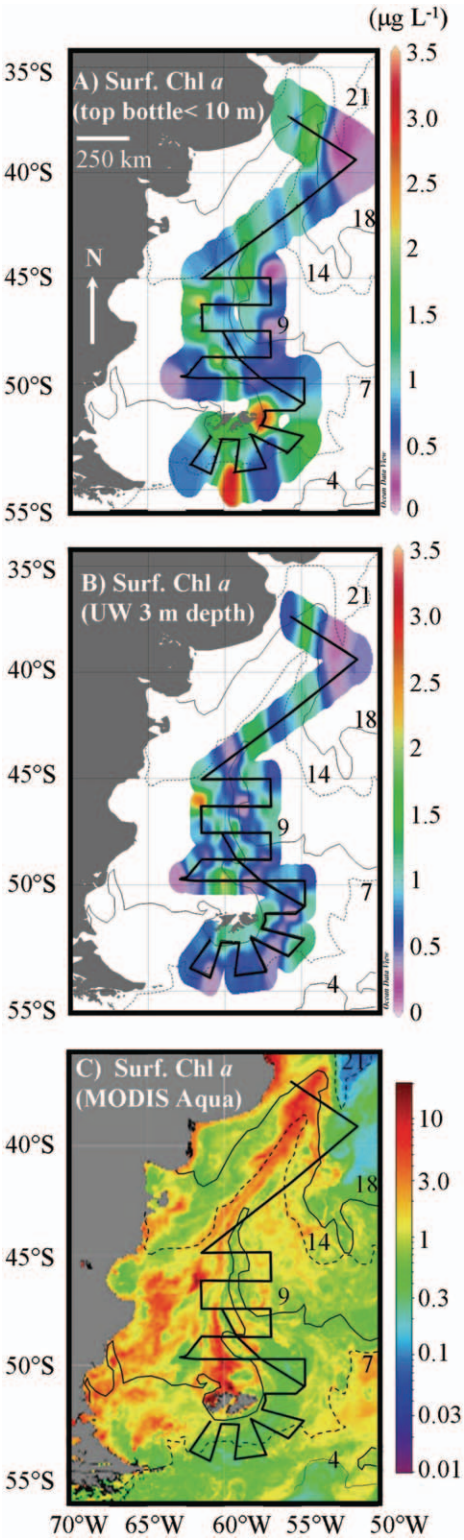

Fig. 3. (A) Chl *a* concentration (from surface bottle measurements; μg chlorophyll L^{-1}). (B) Chl *a* concentration derived from continuous surface underway (UW) fluorescence measurements aboard ship, calibrated to 73 discrete chlorophyll samples taken from UW flow during expedition. Least squares power function for predicting chlorophyll concentration from fluorescence was: y(± 0.208) = 0.3907(± 0.0358) × 0.5418(± 0.058); r^2 = 0.551; F_{73} = 86; $p < 0.001$; data not shown). (C) MODIS-Aqua-derived Chl *a* concentration from December 2008 (9 km, monthly binned data). In all panels, the cruise track is overlaid (heavy black line). Finer solid and fine dashed lines outline the SST fronts as seen in Fig. 2A.

distributions, with greatest concentrations up to 1 μmol L^{-1} in the 7–9°C water, particularly in the core of the coccolithophore bloom and over the Patagonian Shelf (Fig. 5B). The relative pattern of phosphate (not shown) paralleled nitrate (Fig. 5A), with highest concentrations in the FC south of the FIs (1.5 μmol L^{-1}), gradually decreasing to 0.75–1.0 μmol L^{-1} in the most intense parts of the bloom in the FC, then decreasing to 0.1 μmol L^{-1} further north in the Brazil Current. Silicate concentrations were depleted below 1 μmol L^{-1} within the FC. The only surface waters highly elevated in silicate were at the west end of Line A (waters influenced by the Rio de la Plata) and east end of Line A (Brazil Current waters), as well as the eastern end of line G and the north end of line H (east of the coccolithophore-rich waters; Fig. 5C). The ratio of total dissolved inorganic nitrogen (DIN = nitrate + nitrite + ammonium) to dissolved inorganic phosphorus (DIP) showed values of 13 in the FC south and east of the FIs (i.e., below the Redfield ratio of 16; Fig. 5D), situated in the highest density water (Fig. 2D). The DIN : DIP ratio continued to drop in the northern part of the study region. Through the core of the FC, nitrate represented > 90% of the available DIN in waters < 14°C (Fig. 5E).

Residual nitrate was calculated as the difference between the molar concentrations of nitrate minus silicate (Townsend et al. 2010). Thus, the greater the residual nitrate, the less silicate was available for diatoms for growth and cell division relative to other phytoplankton that do not require silicate (e.g., coccolithophores). Residual nitrate declined toward the north in the core of the FC (Fig. 5F).

Continuous underway observations—Results from the continuous underway inherent optical property sampling showed differential effect of the coccolithophores on particulate backscattering and scattering in waters of the Patagonian Shelf. Whereas particulate backscattering (b_{bp}) showed peaks associated with the main axis of the coccolithophore bloom and a dinoflagellate bloom (*Prorocentrum* sp.; ~ 60°W 50°S; Fig. 6A), the particulate scattering (b_p) at 531 nm showed a peak only for the bloom of the dinoflagellate *Prorocentrum* sp. (Fig. 6B). The backscattering probability ($b_b^{\sim} = b_{bp}(b_p)^{-1}$) showed elevated values of ~ 2% within the main axis of the coccolithophore bloom, whereas the values in the dinoflagellate bloom were < 1% (Fig. 6C). In the Brazil Current water (characterized by warm temperatures and low b_{bp}; Fig. 6A), $b_b^{\sim}$ was also as high as 2% (Fig. 6C). The chlorophyll-specific absorption (a_p^*) was calculated (Fig. 6D) from the a_{p440} measurements and underway Chl *a* (underway fluorescence calibrated with discrete Chl *a* measurements). However, some of the data were unusable due to bubbles in the flow of the absorption tube of the ac-9

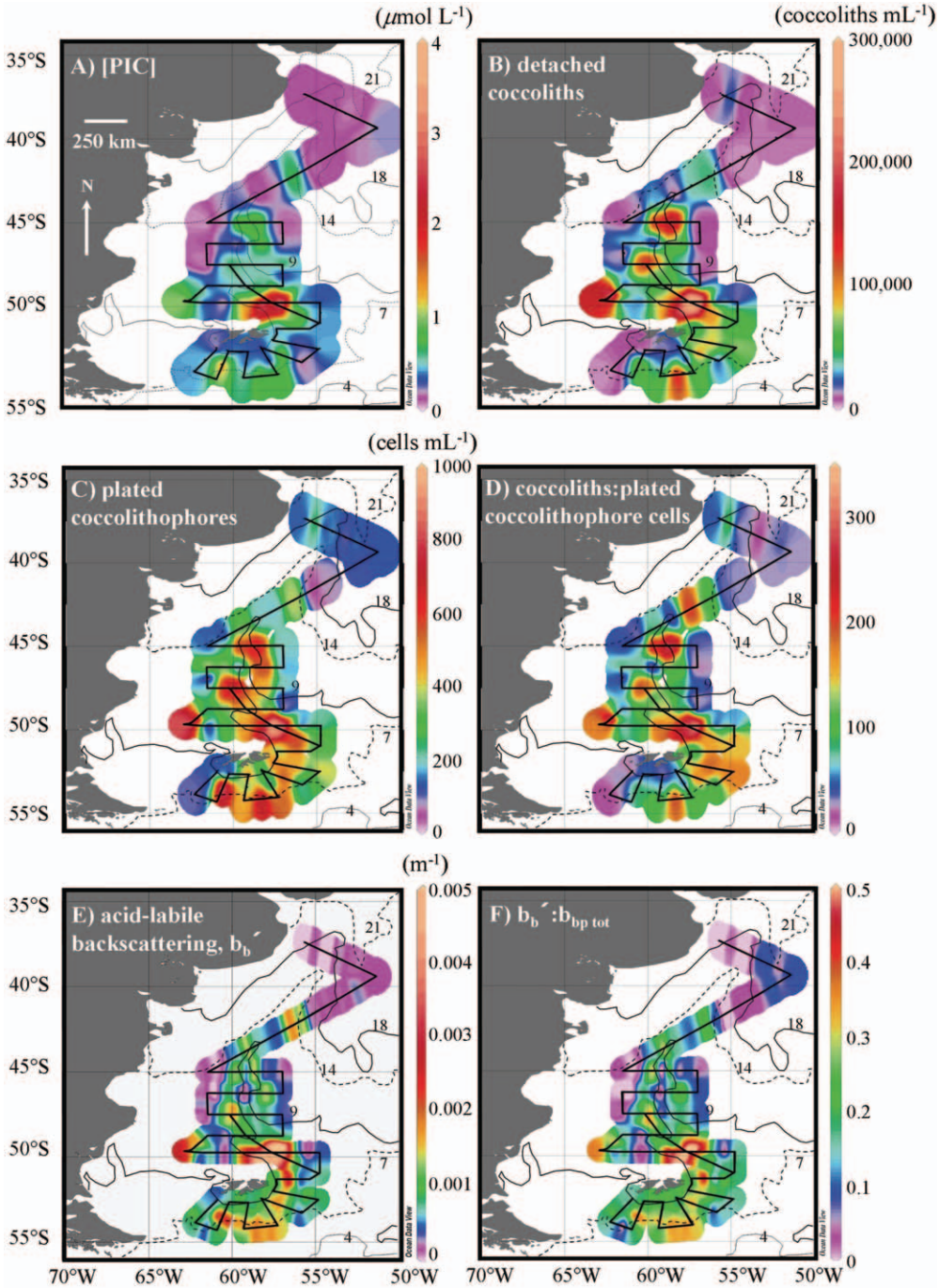

Fig. 4. Concentrations of PIC and coccolithophores and associated optical backscattering in the Patagonian Shelf coccolithophore bloom. (A) ICP–OES measurements of particulate calcium, converted to PIC concentration (μmol L^{-1} or mmol m^{-3}). (B) Coccolith concentration (per milliliter) measured using birefringence microscopy. (C) Concentration of plated coccolithophore cells plus coccolith aggregates (per milliliter). (D) Ratio of detached coccoliths to plated coccolithophores. (E) Continuous underway data for acid-labile backscattering (b'_b; that backscattering which disappears upon the dissolution of aragonite and calcite). (F) Fraction of total backscattering contributed by acid-labile backscattering $(b'_b(b_{bp})^{-1})$. Cruise track is overlaid on all six panels along with contours of the SST. In all panels, the green, orange, and red regions represent the central portion of the highly reflective coccolithophore-rich water. Two different coccolithophore blooms were observed, one to the northeast of the Falkland Islands over the main axis of the FC and one over the Argentine continental shelf (west part of survey area).

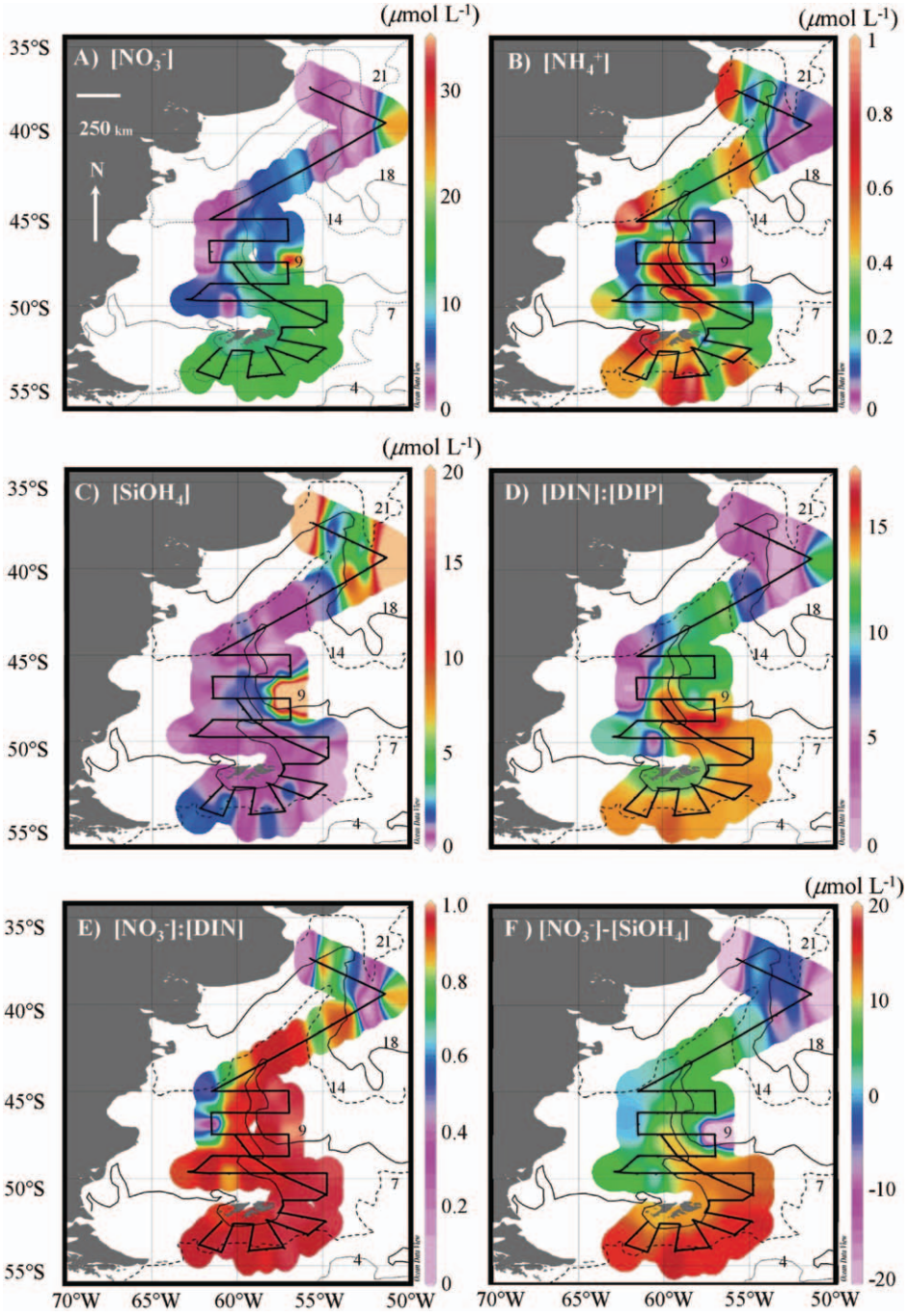

Fig. 5. Nutrient patterns over the Patagonian Shelf region during COPAS'08. (A) Nitrate concentration (μmol L^{-1}), (B) ammonium concentration (μmol L^{-1}), (C) silicate concentration (μmol L^{-1}), (D) molar ratio of total DIN (nitrate, nitrite, ammonium) to dissolved inorganic phosphorus, (E) molar ratio of nitrate to total DIN, and (F) residual nitrate (nitrate concentration − silicate concentration; μmol L^{-1}). In all panels, the cruise track is overlaid (heavy black line) for reference.

and are not reported here. The data showed that $a^*_{p\,440}$ values were 0.04 to 0.06 m^2 (mg Chl *a*) $^{-1}$ in the main axis of the bloom, with higher values of 0.1–0.2 m^2 (mg Chl *a*) $^{-1}$ on the western side of the survey area (Fig. 6D). Absorption of colored dissolved organic matter (CDOM) and detritus (a_{pg412}; Fig. 6E) showed highest values in the waters of the northern part of the survey area, with warm (> 18°C), fresh (< 31), low-density (< 23.5 sigma–theta) water of the Rio de la Plata (Fig. 2A,C,D). CDOM absorption values within the main axis of the coccolithophore bloom were the lowest of the entire cruise (Fig. 6E, *see* waters south of the FIs). Similarly, the slope of the absorption spectrum between 412

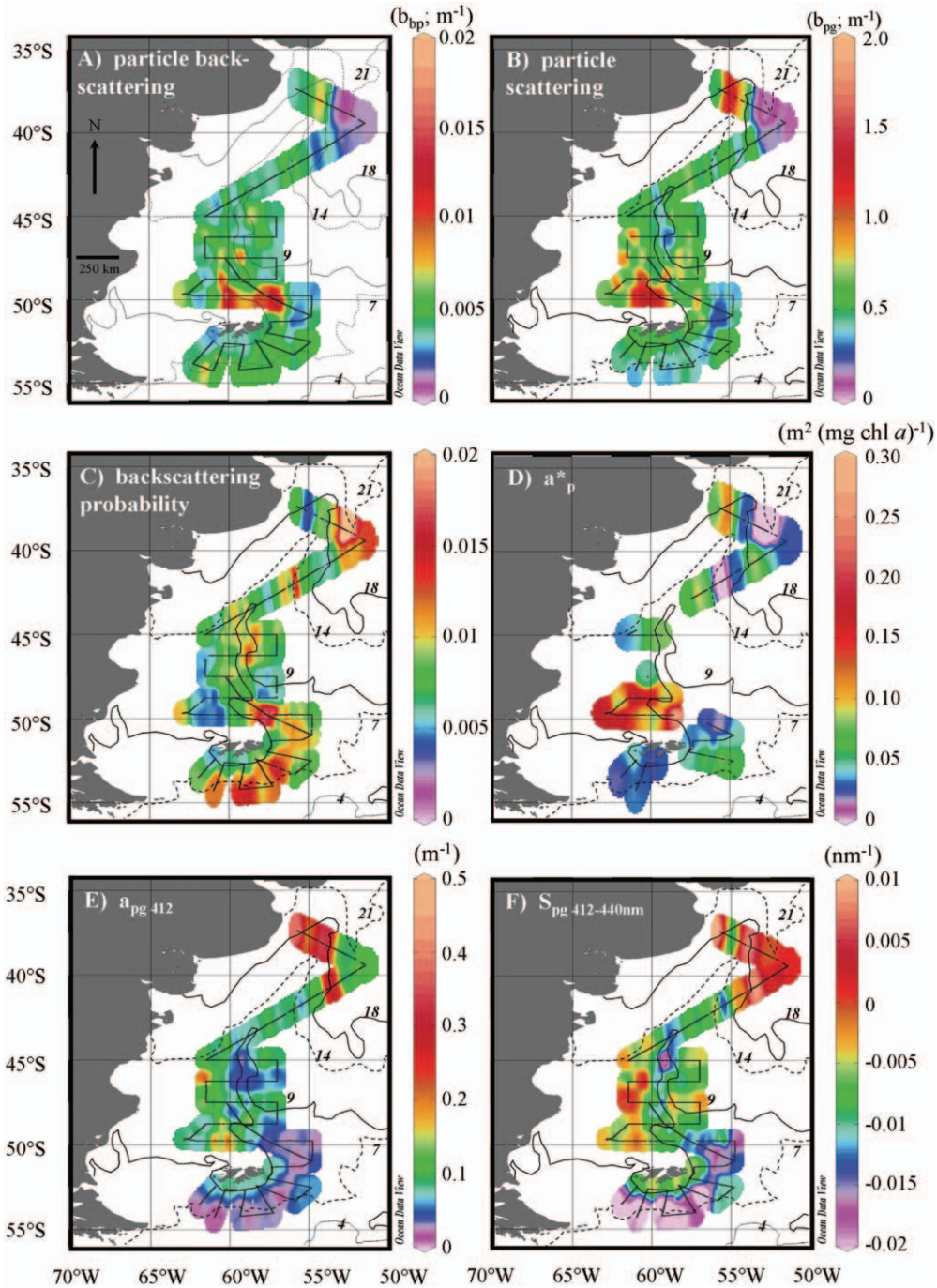

Fig. 6. Surface bio-optical properties over Patagonian Shelf study area (A) b_{bp} (m^{-1}; 531 nm); (B) b_{pg} (m^{-1}; 531 nm); (C) $\tilde{b_b}$ (531 nm); (D) a^*_p (m^2 [mg Chl a]$^{-1}$; 440 nm); (E) a_{pg} (m^{-1}; 412 nm); (F) S_{pg} (412–440 nm).

and 440 nm for combined dissolved and particulate (detrital) matter (S_{pg}) was steeply negative in the main axis of the coccolithophore blooms south of the FIs (Fig. 6F), with slopes becoming less negative as the FC flowed northwestward, north of the FIs. Positive slopes (S_{pg} 412–440) were observed in the clearest water seen on the trip, within the Brazil Current (Fig. 6F), even though overall dissolved and detrital absorption levels were moderate (Fig. 6E).

Particle properties and their variability with residual nitrate—Biogenic silica (BSi; associated with diatom frustules) was present at low values (< 600 nmol L^{-1}) inside the coccolithophore bloom. BSi concentrations increased to the east of the coccolithophore bloom, which wrapped around the FIs (Fig. 7A). The only region with elevated values of BSi was in the surface waters on the nearshore end of Line A, in low-salinity waters (Fig. 2C)

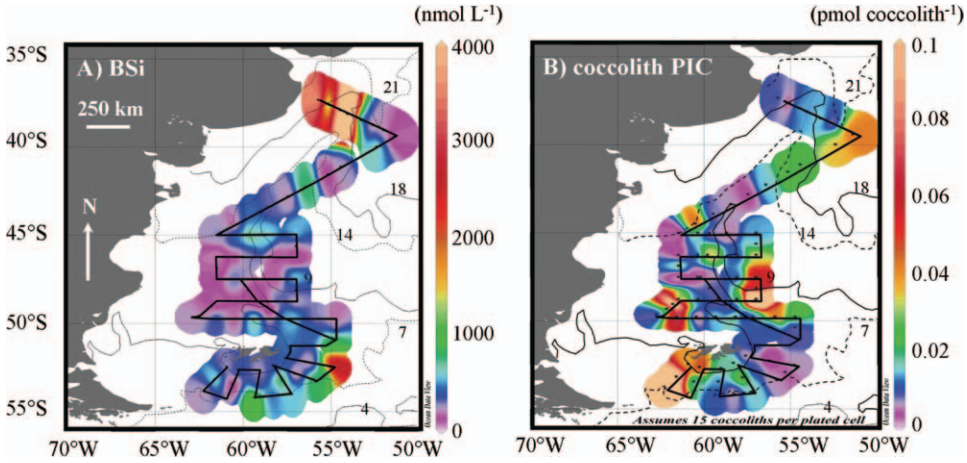

Fig. 7. (A) Biogenic silica distribution through the study area (BSi; nanomol L^{-1}). (B) PIC per coccolith estimated by normalizing the total PIC concentration to the sum of detached coccoliths plus the number of plated cells × 15 (assuming each cell has 15 coccoliths).

influenced by the Rio de la Plata. High BSi concentrations were also observed in surface waters at the intersections of lines R and S. High-salinity Brazil Current waters (east end of line A) showed extremely low values of BSi (< 100 nmol L^{-1}; Fig. 7A).

The calcite mass per coccolith was calculated by normalizing the PIC concentration to the sum of the detached coccolith concentration (birefringent "quads"; considered the least ambiguous identifier for detached coccoliths) and the plated cell concentration multiplied by 15 (assuming that each plated cell had 15 coccoliths). Within the region of the center of the bloom, the PIC per coccolith was 0.008–0.017 pmol PIC per coccolith (Fig. 7B). The mean (± standard deviation) PIC per coccolith overall was 0.022 (± 0.036) pmol PIC per coccolith; $n = 81$. A histogram of the PIC per coccolith (not shown) indicated that ~ 85% of the values were < 0.017 pmol PIC per coccolith, with a bimodal distribution, with peaks at ~ 0.007 and 0.012 pmol PIC per coccolith, positively skewed with a small number of measurements ($n = 10$) between 0.033 and 0.083 pmol PIC per coccolith.

Residual nitrate concentrations showed strong latitudinal variability (positive values from 55°S to 45°S and zero or negative values further north; Fig. 8A). Highest values of residual nitrate over the top 20 m were observed between 5°C and 12°C, at which temperature coccolith concentrations, plated cell concentrations, PIC, and PIC : POC were most elevated (Fig. 8B–D,F). Highest PIC per coccolith (Fig. 8E), in contrast, was observed at temperatures above 12°C, at which residual nitrate was close to zero. Lowest BSi concentrations and FlowCAM-derived diatom biomass were observed between 5°C and 12°C, whereas elevated BSi and diatom biomass was observed in waters warmer than 12°C, in which residual nitrate was negative (i.e., silicate > nitrate; Fig. 8G,H).

Time series of remotely sensed properties at four sites—The time series of the remote sensing product for Chl *a* concentration, SST (11 μm band), and PIC concentration (merged two-band, three-band PIC algorithm) were examined at four sites in the study area using MODIS Aqua data, focused on nine pixels centered at the numbered locations shown in Fig. 1. Two patches had high-reflectance *E. huxleyi* blooms (patch 1 was from a small, bright coccolithophore feature at the western end of line L, and patch 4 was the largest high-reflectance feature in the region on line L at 58°W). Two patches were dominated by the dinoflagellate *Prorocentrum* sp. (both at 60°W, one on line G and one on line L). SST followed the same pattern at all stations, with two SST maxima, one in early December and a broader SST maximum between February and March. All regions showed one or several peaks in Chl *a* between mid-September and early December, with low (or negligible) PIC (we hereafter refer to these populations as being dominated by noncalcifying phytoplankton). Highest PIC concentrations were observed in early December 2008, following the period dominated by noncalcifying phytoplankton. In all cases, the largest PIC peak fell in the same 8 d period on 28 November 2008, synchronous with the first SST peak (this was true even in the *Prorocentrum* sp. patches). Following the period of peak PIC concentration in each subregion, PIC concentrations declined gradually during the subsequent 2–3 months, as surface waters warmed and then cooled during February and March. The only time that high PIC was seen together with elevated chlorophyll was in the southerly *Prorocentrum* sp. bloom (patch 3; Fig. 9C).

Discussion

Comparison of bloom observations with previous studies—The Patagonian Shelf coccolithophore bloom observed in December 2008–January 2009 was roughly constrained to the 7–9°C, 33.9 salinity, high-density water of the FC, situated along the shelf break front (Painter et al. 2010; Poulton et al. 2011). Highest reflectance and densest coccolithophore populations observed in this study were found well east of the January 2008 Patagonian Shelf coccolithophore ship and satellite observations of Garcia

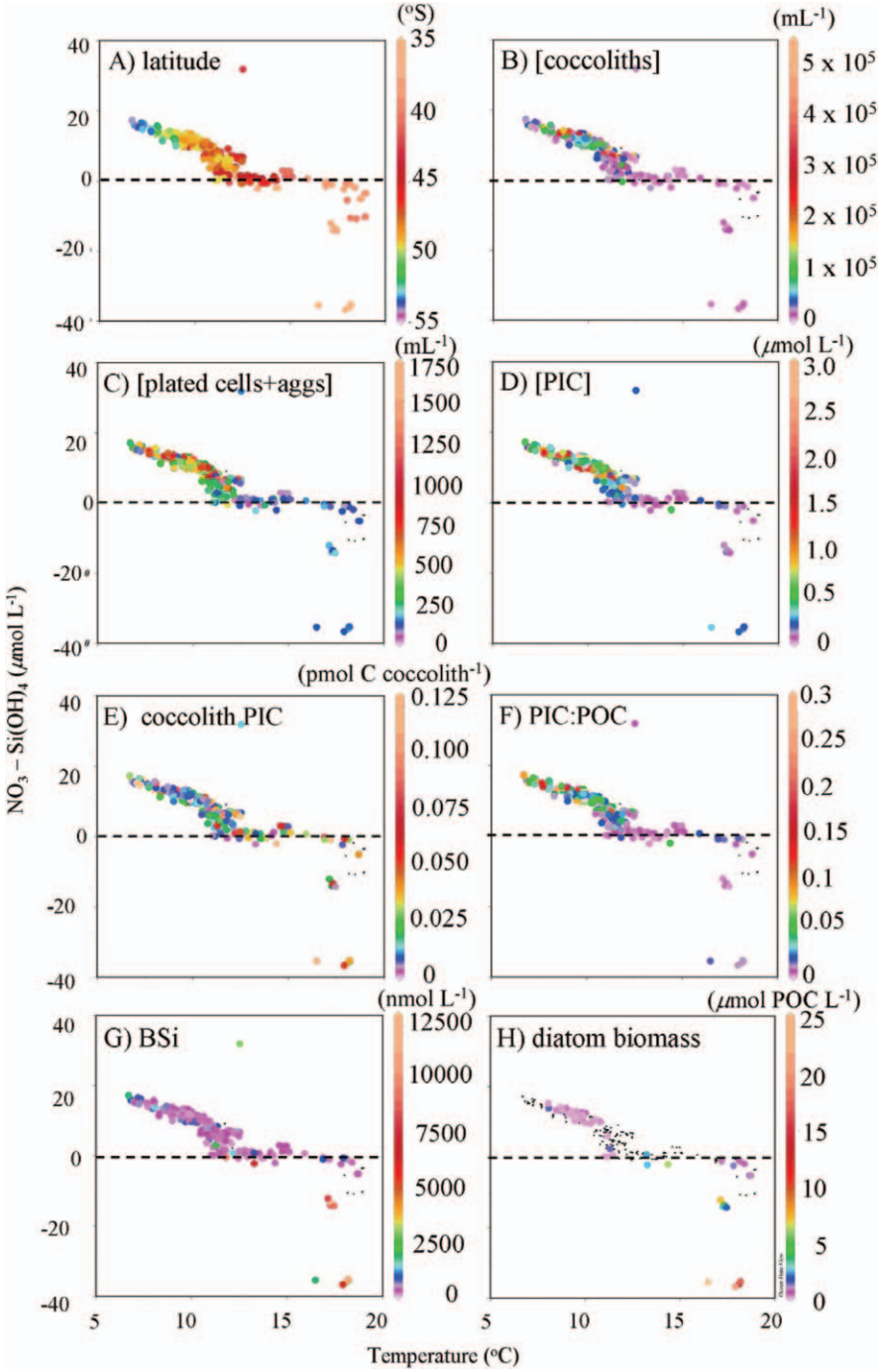

Fig. 8. Residual nitrate in the surface 20 m of the water column as a function of temperature from COPAS'08, with different variables shown as the color of the dots: (A) latitude, (B) coccolith concentration (per milliliter), (C) concentration of plated coccolithophores and coccolith aggregates (aggs. per milliliter), (D) PIC concentration (μmol L^{-1}), (E) PIC per coccolith (pmol $coccolith^{-1}$), (F) PIC : POC ratio, (G) biogenic silica (nmol L^{-1}), and (H) diatom biomass (μmol POC L^{-1}).

et al. (2011) and de Souza et al. (2012) and were more consistent with the satellite observations of the 2004 coccolithophore bloom described by Signorini et al. (2006). Based on hydrographic observations, the association of the coccolithophores with the cold, dense waters of the FC (south and north of the FIs; Painter et al. 2010; Poulton et al. 2011) would suggest that there is some factor (or factors) associated with the FC that encourages their growth. These could be either bottom-up factors (such as a limiting nutrient, mixed layer depth, or irradiance) or

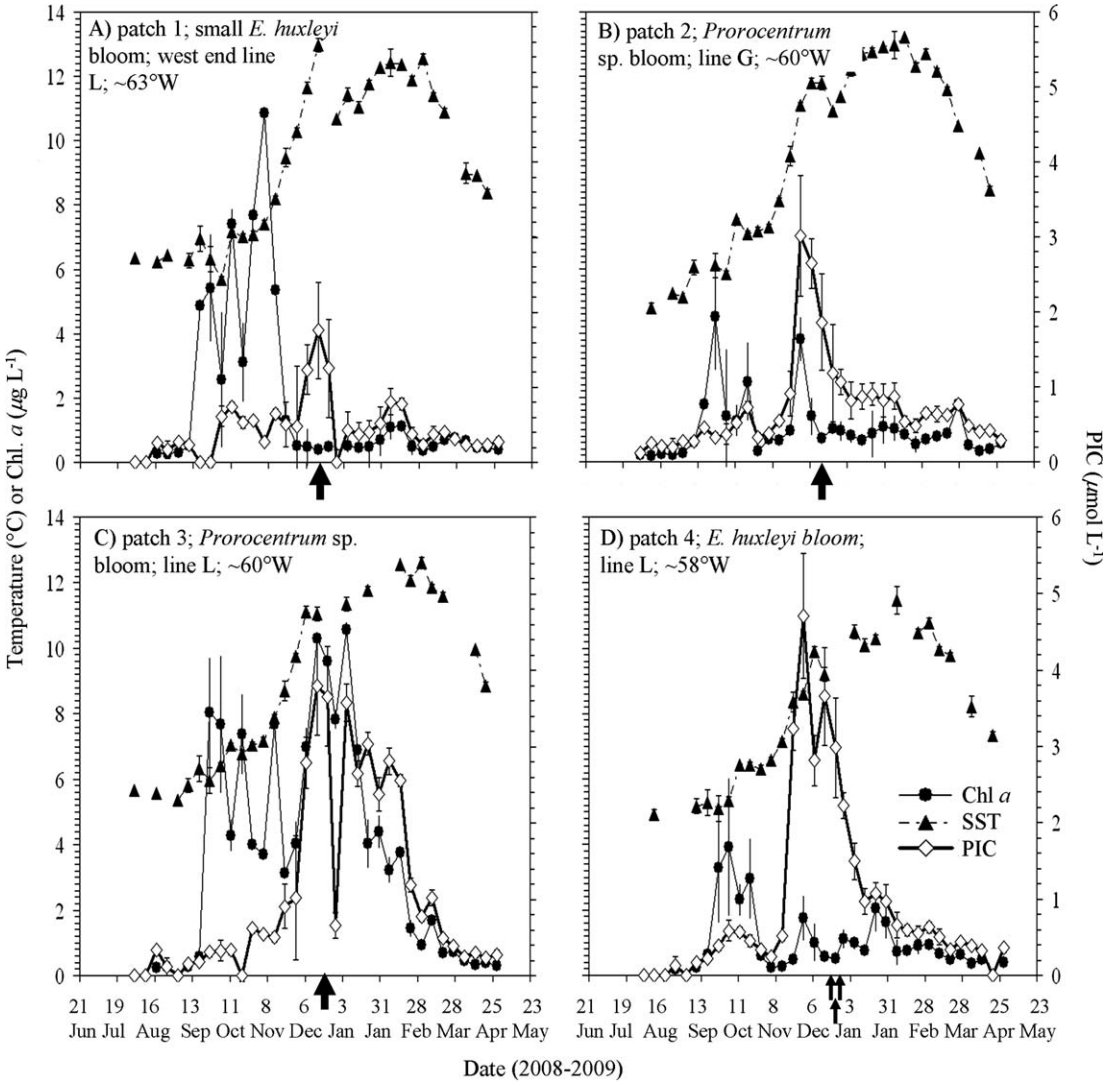

Fig. 9. Remotely sensed time series for four regions of study area for sea surface temperature (°C), Chl *a* (μg L^{-1}), and PIC concentration (μmol L^{-1}), running from June 2008 to April 2009. (A) Patch 1, small *Emiliania huxleyi* bloom at west end of line L, near Sta. 68 on 18 December 2008 (image pixels centered at 49.75°S, 062.83°W). (B) Patch 2, *Prorocentrum* sp. bloom on line G, near Sta. 46 on 14 December 2008 (image pixels centered at 47.50°S, 060.21°W). (C) Patch 3, *Prorocentrum* sp. bloom on line L between Sta. 72 and 73 on 19 December 2008 (image pixels centered at 49.75°S, 060.18°W). (D) Patch 4, main *E. huxleyi* bloom centered on line L sampled at Sta. 72, 90, and 106 on 19, 22, and 24 December 2008, respectively (image pixels centered at 49.75°S, 057.65°W). All data are 8 d averages with standard deviation error bars. Average area of each patch is 9 km × 9 km. Arrows below each *x*-axis show the 8 d average, which includes the dates that the ship occupied each patch.

ecological factors related to competition or predation (e.g., the absence of competing diatoms or lack of grazing by copepods). Patches of elevated ammonium in surface waters within the bloom (Fig. 5B) suggest that grazers were present, producing significant regenerated nitrogen, although nitrate still represented > 90% of the DIN in these waters (Fig. 5E).

Inshore of the main core of high-reflectance water in the FC, there were several bands of chlorophyll-rich water interspersed with lower coccolithophore waters (Figs. 1, 3C). This was similar to satellite ocean-color images published by others (Signorini et al. 2006; Garcia et al. 2011; de Souza et al. 2012). Romero et al. (2006) attributed these bands to bottom-trapped tidal fronts induced by tidal dissipation on the shelf. The bands consist of well-mixed water (high-chlorophyll waters) with intervening waters that were more stratified. Romero et al. (2006) observed a shelf break maximum in satellite-derived chlorophyll extending from 37°S to 51°S with two inner-shelf elevated-chlorophyll regions off of the Valdes Peninsula (42°S, 64°W) and along a band closer to the coast from 46°S to 52°S. The smaller subordinate bloom of coccolithophores (PIC-rich waters) seen on the west end of line L in our study was likely associated with one such band of stratified water between two such tidal fronts (but note that those waters were not as concentrated with PIC as those further east on line L, northeast of the FIs, at the intersection of line N). Moreover, the western coccolithophore feature that

we observed was probably similar to the feature described by Garcia et al. (2011) and de Souza et al. (2012).

Chl *a* concentration measured by ship and satellite (Fig. 3) suggested moderately low chlorophyll levels (0.3–0.6 μg L^{-1}) in the core of the coccolithophore bloom and core of the FC (where the FC location was determined by the ship's acoustic doppler velocity measurements, south, east, and north of the FIs; Painter et al. 2010). Such concentrations are completely consistent with previous observations of other coccolithophore blooms, where "bloom" is a misnomer because they are not characterized by high biomass, but rather by low-to-moderate biomass and with a striking change in reflectance due to the high concentrations of detached PIC coccoliths (Holligan et al. 1993). These levels were consistent with Chl *a* levels observed in previous Patagonian Shelf coccolithophore blooms, documented using remote sensing or ship-based measurements over the east Patagonian Shelf at 50°S (Signorini et al. 2006; de Souza et al. 2012). Chlorophyll levels observed in this work were slightly lower than those reported by Garcia et al. (2011; *see* their fig. 5A; Sta. 503, 504).

There were strong similarities in the spatial patterns of the various indices of coccolithophore abundance, including concentration of PIC, coccoliths, coccolithophores, and acid-labile backscattering (Fig. 4). Again, these results showed that the core of the coccolithophore bloom was in the FC. However, these in-water measurements showed the concentration of plated coccolithophores to be uniformly high around the east side of the FIs (Fig. 4A–C, E). Indeed, concentrations of plated coccolithophores were about 1000 cells per milliliter, much lower than the peak value of 11,000 plated coccolithophores per milliliter observed by Garcia et al. (2011). Based on previously published values of the Chl *a* per cell for *E. huxleyi* (0.26 pg $cell^{-1}$; Haxo 1985) 1000 cells per milliliter would have produced a Chl *a* concentration of $\sim$ 0.26 μg L^{-1}, which was representative of our Chl *a* observations as well as those of others. However, the estimate of 11,000 *E. huxleyi* cells per milliliter of Garcia et al. (2011) should have produced Chl *a* concentrations of 2.6 μg L^{-1}, $\sim$ 5 times higher than the Chl *a* concentration that they actually observed. Detached coccoliths exceeded 250,000 per milliliter northeast of the FIs (Fig. 4B), with ratios of detached coccoliths to plated cells of $>$ 300 (Fig. 4C). Such coccolith : cell ratios are representative of the sorts of ratios observed in late-phase coccolithophore blooms (Holligan et al. 1993), higher than the assumed ratios cited by Garcia et al. (2011) of five to six coccoliths per plated coccolithophore cell, which are more characteristic of nonbloom coccolithophore populations. The calcite per coccolith values that we observed were in the low range for *E. huxleyi* coccoliths in general, but they agreed with values for *E. huxleyi* coccoliths determined using scanning electron microscopy (SEM) of B and C morphotypes in the same bloom (0.011–0.026 pmol PIC per coccolith; Poulton et al. 2011).

Bio-optical variability—The bio-optical data for inherent optical properties (IOPs) showed strong differences between particulate backscattering and particulate scattering distributions. Particles that scatter light most efficiently (assuming a refractive index of 1.05, close to that of organic carbon in phytoplankton) have diameters of 1–10 μm (Morel and Ahn 1991). As the diameter increases above 10 μm, particle scattering decreases such that particles from 10 to 100 μm have lower scattering efficiencies; and, at a particle diameter $>$100 μm, such particles contribute little to total particle scattering. The bloom of *Prorocentrum* sp. (20 μm diameter cells) to the west of the coccolithophore bloom on line L (patch 3; Fig. 1) would have qualified as efficient particle scatterers using this criterion. In contrast, they would have been inefficient backscatterers because the most efficient backscatterers are small particles in the diameter range of 0.1–0.4 μm for organic particles with a refractive index of 1.05 (Morel and Ahn 1991).

Calcium carbonate coccoliths (with a diameter of 2–4 μm diameter and relative refractive index = 1.19) would be highly efficient backscatterers (Aas 1981). The plated cell contribution to optical scattering can be greater than the sum of the coccoliths covering them (Voss et al. 1998). The observed elevated backscattering probability in the Patagonian Shelf coccolithophore bloom would be expected for these highly refractive mineral particles, which, in the case of the 2008 coccolithophore bloom, was confined to the main axis of the FC (Fig. 6C). Garcia et al. (2011) observed backscattering probabilities at 660 nm, averaging 2.3% $\pm$ 0.9% in the region to the west of line L, about the same that we observed at 531 nm in the same geographic region, as well as in the core of the FC coccolithophore bloom (Fig. 6C). Ultimately, the different aerial distributions of total particle backscattering and total scattering (Fig. 6A,B, respectively) probably resulted from the fact that *Prorocentrum* sp. and *E. huxleyi* both contributed significant backscattering, whereas the large *Prorocentrum* sp. cells contributed more to total scattering.

Chlorophyll-specific absorption is determined by the extent of pigment packaging and type of pigment (Bricaud et al. 1983). Moreover, there is an inverse linear relationship between $a^*_{p\,440}$ and the product of intracellular pigment concentration and cell diameter (Bricaud et al. 1983). Chlorophyll-specific absorption has been measured before for the dinoflagellate *Prorocentrum* sp. in the laboratory (Stæhr and Cullen 2003) as well as in a bloom in Chesapeake Bay (Gallegos and Bergstrom 2005). Maximal values of $a^*_{p\,440}$ in culture are $\sim$ 0.058 m^2 (mg Chl *a*)$^{-1}$, depending on light and nutrient conditions (Stæhr and Cullen 2003), which is less than the $a^*_{p\,440}$ values observed here (Fig. 6D). Elevated $a^*_{p\,440}$ (values as high as 0.15–0.25 m^2 [mg Chl *a*]$^{-1}$) seen in the *Prorocentrum* sp. bloom on the Patagonian Shelf might have resulted from large amounts of photoprotective pigments in these summer populations, as previously suggested by Ferreira et al. (2009) for the region towards the west of our line L.

As expected, the waters influenced by the Rio de la Plata showed the highest contribution of CDOM and detrital particulate absorption (a_{pg412}; Fig. 6E). The low values of a_{gp412} found in the FC south of the FIs as well as northeast of the FIs were contrary to the CDOM concentrations expected from the global predictions of Siegel et al. (2002),

who suggested that Southern Ocean CDOM concentrations would have been elevated, primarily due to low photobleaching at these high latitudes. The slope, S, of the CDOM absorption between 412 nm and 440 nm was between -0.01 nm^{-1} and -0.02 nm^{-1}, within the core of the *E. huxleyi* bloom (Fig. 6E), suggesting that, for the small amount of CDOM that was present, it was moderately colored. Thus, our results indicate that these populations were releasing minimal CDOM on their own. It is important to note that there are also sources of CDOM north and west of the FIs, over the shelf (Fig. 6E). Garcia et al. (2011) previously showed that, in that same region, mean CDOM absorption accounted for 20.5% of total mean (particulate plus dissolved) absorption at 440 nm (*see* their table 1).

The Patagonian Shelf coccolithophore bloom and nutrient variability—The concentrations of detached coccoliths and PIC decreased as the FC moved northward from the bloom centered at the intersections of Lines L and N (Fig. 4). As mentioned previously, the reasons for this may be related to bottom-up control (nutrients), top-down control (loss of PIC-producing cells via grazing or viral lysis), sinking, or lateral mixing of the bloom with adjacent nonbloom waters. Whereas nitrate concentrations also declined as the FC moved northward (Fig. 5A; Painter et al. 2010), the concentrations still remained relatively high (15 μmol L^{-1}). Such high nitrate concentrations, combined with the low Chl *a* concentrations, indicate that these were HNLC waters (Poulton et al. 2013). With such a low percentage of regenerated nutrients (Fig. 5E), based solely on DIN, these waters should have been able to support significant new production and export. However, the extremely low silicate values (Fig. 5C) suggested that growth of large diatoms was limited, at least in the FC. The fact that the BSi maxima were outside of the FC, southeast of the FIs (Fig. 7A), supported this contention. Brandini et al. (2000) showed silicate data from three November cruises in the 1990s near the location of the main coccolithophore bloom (patch 4; 49.75°S, 057.65°W). Their results showed late-spring concentrations of silicate of 4–8 μmol L^{-1}, well above the concentrations that we measured in December. Their results, combined with the time series of SST, chlorophyll, and PIC at this same site (Fig. 9), support the idea of silicate draw-down by diatoms earlier in the growth season, prior to the main coccolithophore bloom. Finally, nitrogen appeared to be preferentially used relative to phosphorus as the water flowed northward, given that the N : P molar ratio dropped below Redfield ratios by the time the water traversed well north of the coccolithophore bloom (Fig. 5D; Painter et al. 2010). This would suggest that phytoplankton growth continued in the northward-flowing FC.

Do diatoms and coccolithophore co-exist in HNLC waters?—The *E. huxleyi* bloom observed over the Patagonian Shelf, whether north or south of the FIs, was in HNLC waters, with large diatoms dominating only at the periphery of the bloom, again suggesting some sort of competitive relationship between coccolithophores and diatoms. One exception to this observation was south of the FIs, over Burdwood Bank. In these waters with highly abundant nitrate, Redfield N : P ratios, and low silicate (Fig. 5), we observed the co-occurrence of giant diatoms, tentatively identified as *Rhizosolenia castracanii*, as well as the coccolithophore *E. huxleyi*. The *R. castracanii* was noted first, as it was possible to see the large cells on the filter pads without aid of magnification. Over Burdwood Bank, the presence of massive numbers of this diatom were associated with CTD fluorometer traces that were extremely noisy (not shown). This diatom is highly buoyant and is responsible for floating mats (Villareal 1988). *Rhizosolenia castacanii* has been previously observed at high Chl *a* concentrations ($>$ 20 μg L^{-1}) in patches hundreds of kilometers long, along the boundary between the North Equatorial Counter Current and the South Equatorial Current, in the Equatorial Pacific (Yoder et al. 1994). Their buoyancy allows them to accumulate at convergent fronts. Indeed, over Burdwood Bank there was a strong thermal front observed at the 7°C isotherm (Fig. 2A), situated just north of line V (Figs. 1, 2A). This, combined with the northward 50 cm s^{-1} currents flowing towards that hydrographic front (measured with Acoustic Doppler Current Profiler; Painter et al. 2010), suggest the presence of a convergent front. *E. huxleyi* could have accumulated at the same place, given the extraordinary amount of lipids that these coccolithophores produce, some 60% of their total carbon (Fernández et al. 1996), which would confer buoyancy. To our knowledge, this is the first noted instance of the presence of giant diatoms and coccolithophores as co-dominants in the same waters.

Another exception to the idea that diatoms and coccolithophores did not co-exist in the coccolithophore bloom was documented in the same feature through SEM; with a small (5–10 μm) polar diatom of the genus *Fragilariopsis* sp. in concentrations almost as high as *E. huxleyi* (0.2–2 $\times$ 10^3 mL^{-1}), which was estimated to contribute up to $\sim$ 30% of the primary production and carbon biomass (Poulton et al. 2013). This small *Fragilariopsis* sp. would not have been readily identifiable in the FlowCAM due to their small cell size (and the magnification used), but was easily visible in SEM images.

It has been shown previously that small diatoms respond differently to iron addition than do medium and large diatoms. For example, in another HNLC region, the Equatorial Pacific, small pennate diatoms (*Pseudonitzschia* sp.) co-existed with coccolithophores and grew at low iron concentrations, whereas larger diatom cells could not (Brzezinski et al. 2011). In iron- and silicate-addition mesocosm experiments in the Equatorial Pacific, the medium-sized diatoms (20–40 μm cells), and especially the large diatoms ($>$ 40 μm cells), had a strong growth response 120 h following iron addition and an even stronger response if both iron and silicate were augmented together. Small diatoms ($<$ 10 μm) and coccolithophores, on the other hand, did not respond to either iron or silicate additions (Brzezinski et al. 2011). Analogous to our COPAS'08 observations, if the FC was indeed iron-limited, then the *E. huxleyi* and *Fragilariopsis* sp. appeared able to continue growth to the exclusion of larger diatoms.

Residual nitrate and bloom formation—Residual nitrate ($[NO_3^-] - [Si(OH)_4]$; Townsend et al. 2010; Fig. 5F) showed the extent of silicate limitation relative to nitrate and mirrored the relative distribution of N : P (compare Fig. 5D,F). These data suggest that coccolithophores had reduced resource competition with medium and large diatoms within the core of the bloom. Such shifts in residual nitrate have been observed to affect the succession between dinoflagellate vs. diatom-dominated phytoplankton populations in other shelf environments (e.g., Gulf of Maine ecosystem; Townsend et al. 2010). Residual nitrate in the surface 20 m varied strongly with temperature throughout the study area (Fig. 8). Concentrations of detached coccoliths, plated coccolithophore cells, PIC, and PIC : POC all showed highest values when the residual nitrate was positive (with strong silicate draw-down; Fig. 8B–D,F). Coccoliths containing the most PIC also were seen in waters with residual nitrate that was slightly positive to negative. Interestingly, this is also where morphotype A coccoliths with higher calcite content were more abundant along the Patagonian Shelf (Poulton et al. 2011).

Consistent with there being a competitive relationship between coccolithophores and medium to large diatoms, BSi and diatom biomass was highest when the residual nitrate was negative (i.e., when silicate > nitrate; Fig. 8G,H). Similar inverse relationships were observed in the equatorial Pacific HNLC waters, in which calcification was inversely correlated to the production of biogenic silica in nutrient-addition experiments with iron, silicate, or both (Brzezinski et al. 2011). Such results are roughly consistent with the conceptual view of phytoplankton succession, first proposed by Margalef (1978), in which (at least) medium and large diatoms and coccolithophores generally fill different niches in a "mandala" based on the variability of turbulence vs. nutrient availability, predicting that diatom populations give way to coccolithophores as turbulence and nutrient concentrations decline. Small diatoms, however, co-exist with coccolithophores and do not appear to be subject to either iron- or silicate-limitation to the same degree as larger diatoms. Unlike large diatoms, the abundance of small diatoms and coccolithophores is probably strongly controlled by top-down grazing pressure from microzooplankton, which allows them to co-exist in the same middle portion of Margalef's conceptual mandala (Brzezinski et al. 2011).

Factors controlling the Patagonian Shelf coccolithophore bloom—Observations from the COPAS'08 cruise, as well as remote sensing imagery from SeaWiFS and MODIS, suggest that coccolithophores are visible within the FC for 8 months (October to May; albeit, in May, only the northernmost extent is visible, due to low sun angles that limit satellite retrievals), with the peak coccolithophore concentrations centered north and east of the FIs during austral summer. Whereas nutrient and hydrographic data all point to the coccolithophore bloom forming in HNLC water, originating from the Southern Ocean (Figs. 3–5; Painter et al. 2010; Poulton et al. 2013), we cannot confirm whether the ultimate limiting nutrient was iron as has been observed in other Southern HNLC water (Boyd et al. 2000), because no dissolved iron measurements were taken during this study. However, it is noteworthy that iron usage appears to be greatest in waters that receive Patagonian dust and river run-off (Gaiero et al. 2003) and is less where shallow sediment resuspension may be supplying the iron (depths < 500 m; Boyd et al. 2012).

Remotely sensed, true-color images over the Patagonian Shelf have been arranged sequentially into a video loop (*see* Web Appendix: www.aslo.org/lo/toc/vol_59/issue_5/1715a.wmv). The results show that the coccolithophore bloom is well tied to the stratified side of the shelf front, with warmer SSTs (thus, likely on the less mixed, higher stability side of the front). Moreover, there are waters of higher reflectance (i.e., elevated PIC concentrations) that emanate from the main part of the bloom (patch 4; Fig. 1) and are carried along the shelf front at a velocity of ~ 50 cm s^{-1} for the entire 1000 km length of the feature, ultimately advected cyclonically offshore at the confluence of the Brazil Current and FC at 40°S. Due to clouds, it was not possible to determine the frequency at which such pulses of high PIC water were discharged into the FC (e.g., fortnightly or monthly), which would have allowed further insights into the physical driver of these PIC pulses. It is also possible that, if iron were limiting to coccolithophores along this front, such bright features might result from a cyclonic eddy propagated along the shelf front, pulling deep, sediment-derived, iron-rich waters upward as it propagated northward. Regardless, it is clear from the image sequence that PIC generated off the FIs is being pumped northward in pulses, where it is ultimately transported eastward into the subtropical frontal boundary region.

Temporal variability in the diatom, coccolithophore, and dinoflagellate blooms—From an ecological perspective, our overall results point to a combination of physical factors and resource competition between silicifying phytoplankton (specifically medium and large diatoms) and coccolithophores within the FC as influencing the appearance of the *E. huxleyi* blooms. Based on the remote-sensing time series (Fig. 9), the first spring phytoplankton bloom was dominated by noncalcareous phytoplankton (probably large diatoms, but it is difficult to discriminate because the spectral reflectance of diatoms and dinoflagellates are similar). This followed the first warming period during austral spring. Note that there was still a low but measurable increase in PIC concentration in early spring, too.

The major PIC peak at each of the four sites occurred after an extended springtime warming. Such warming likely would have signified increased stability and favored coccolithophores (with their higher affinity for nutrients; Eppley et al. 1969) and dinoflagellates (with their ability to vertically migrate; Olsson and Granéli 1991) over large diatoms (Margalef 1978). The general synchrony in the satellite-observed PIC peaks in the four patches (separated by up to 500 km) attests to forcing over scales of similar, or larger, length. Physical factors (including, but not limited to, low winds, reduced convective mixing, increasing day length, warming through extended periods of elevated solar irradiance, advection; Zondervan 2007) all could have

played a role in this apparent mesoscale and submesoscale growth synchrony. Furthermore, temperature is thought to be a primary factor in regulating coccolithophore growth (Boyd et al. 2010), although the Patagonian Shelf bloom declined with seasonally increasing temperature (Fig. 9C,D; Painter et al. 2010). Moreover, horizontal stirring is critical in defining and maintaining phytoplankton patches in the sea along frontal boundaries (D'Ovidio et al. 2010).

However, as discussed above, nutrients, and the biological response to them, also appeared to play an important role in the distributions of these algal groups (e.g., the preference of the coccolithophores for waters with positive residual nitrate). A number of workers have observed that the end of the diatom bloom in the North Atlantic is associated with silicate depletion (Leblanc et al. 2009). Moreover, there have been previous observations of the subsequent transition from large diatoms to coccolithophores when silicate is exhausted (Leblanc et al. 2009; Boyd et al. 2010). Our results from the Patagonian Shelf are consistent with these controls on coccolithophore growth.

Dense dinoflagellate blooms north of the FIs highlighted the complex factors controlling the bio-optical properties of these shelf waters. Note that coccolithophores co-occurred with dinoflagellates in the two *Prorocentrum* sp. patches shown in Fig. 9B,C (*see* PIC and chlorophyll traces). They were located in warmer (11°C) surface waters with low-silicate, reduced nitrate, and positive residual nitrate (Figs. 5, 6B, 8), away from the core of the HNLC waters of the FC. We conjecture that earlier blooms of large diatoms in October (Fig. 9B,C) drew down the silicate, thus allowing coccolithophores (or small, < 10 μm diatoms) to outcompete the larger diatoms for limiting nutrients. We suspect that vertical migration by *Prorocentrum* sp. (Olsson and Granéli 1991) allowed this dinoflagellate genus to exploit deeper nitrate sources and achieve the high surface cell densities observed, whereas the ability of *E. huxleyi* to grow in the low-iron, HNLC, surface waters allowed them to coexist in the same patches. The optical signal of the coccolithophores was not necessarily from their high biomass but from the high concentrations of coccoliths that were produced and detached.

The horizontal optical gradients described between the dinoflagellate and coccolithophore waters remain some of the strongest ever observed by these authors for open ocean settings and resulted from a dynamic juxtaposition of physical forcing (which affected horizontal and vertical mixing), chemical conditioning by previous diatom growth, and biological response of the nonsilicifiers (including vertical migration of *Prorocentrum* sp. and high nutrient affinity of *E. huxleyi* for iron). All acted to maintain the patches of coccolithophores and dinoflagellates in stable blooms and in close proximity over the Patagonian Shelf for seasonal (or longer) timescales, in agreement with D'Ovidio et al. (2010).

The Patagonian Shelf coccolithophore bloom is by far the brightest part of the GCB. At least as seen in remote sensing imagery, concentrations of PIC within the GCB gradually decline to the east of the Patagonian Shelf through the Atlantic, Indian, Australian, and Pacific sectors of the Southern Ocean (Balch et al. 2005). The association of the GCB coccolithophores with the stable side of frontal boundaries (Balch et al. 2011*a*; plus *see* references in the introductory paragraph) would be consistent with the hypothesis that hydrography (i.e., turbulence) and associated bottom-up delivery of nutrients (i.e., degree of eutrophy) favor coccolithophore growth over diatom growth in the GCB, particularly after surface waters warm in the late spring, a concept that originated with Margalef (1978). Work is currently ongoing to test this hypothesis in the GCB waters eastward of the Patagonian Shelf.

Acknowledgments

We thank the scientific party of Coccolithophores of the Patagonian Shelf (COPAS) 2008 cruise, and the captain and crew of the R/V *Roger Revelle* who expertly operated the ship during this study. We thank D. Schuller (Scripps Institution of Oceanography) for the running of nutrient samples and Norman Kuring (Goddard Space Flight Center, National Aeronautics and Space Administration) who provided real-time satellite imagery to help us steer the ship through the mesoscale coccolithophore bloom over the Patagonian Shelf. We gratefully acknowledge reviews of an earlier version of this paper by Philip Boyd (University of Tasmania) and an anonymous reviewer. Support for this work was provided by the National Science Foundation cruise (Division of Ocean Sciences-0728582; 0961660) to W.M.B. Additional support for this work was also provided by National Aeronautics and Space Administration (NNX11AO72G; NNX11AL93G; NNX10AT67G). Financial support for S.C.P. was provided by the Luminescence and Marine Plankton project funded by the Defense Science and Technology Laboratory under the Joint Grant Scheme program with John T. Allen (proposal reference 1166). A.J.P. was financially supported by a Natural Environmental Research Council postdoctoral fellowship (NE/F015054/1).

References

Aas, E. 1981. The refractive index of phytoplankton. Institute Report Series, No. 46. Univ. of Oslo.

Balch, W. M. 2004. Re-evaluation of the physiological ecology of coccolithophores, p. 165–190. *In* H. R. Thierstein and J. R. Young [eds.], Coccolithophores—from molecular processes to global impact. Springer-Verlag.

———, D. T. Drapeau, B. C. Bowler, E. S. Booth, E. Lyczskowski, and D. Alley. 2011*a*. The contribution of coccolithophores to the optical and inorganic carbon budgets during the Southern Ocean Gas Experiment: New evidence in support of the "Great Calcite Belt" hypothesis. J. Geophys. Res. Special Issue **116:** 1–14.

———, ———, ———, ———, L. A. Windecker, and A. Ashe. 2008. Space-time variability of carbon standing stocks and fixation rates in the Gulf of Maine, along the GNATS transect between Portland, ME and Yarmouth, NS. J. Plankton Res. **30:** 119–139, doi:10.1093/plankt/fbm097

———, ———, T. L. Cucci, R. D. Vaillancourt, K. A. Kilpatrick, and J. J. Fritz. 1999. Optical backscattering by calcifying algae—separating the contribution by particulate inorganic and organic carbon fractions. J. Geophys. Res. **104:** 1541–1558, doi:10.1029/1998JC900035

———, H. R. Gordon, B. C. Bowler, D. T. Drapeau, and E. S. Booth. 2005. Calcium carbonate budgets in the surface global ocean based on MODIS data. J. Geophys. Res. Oceans **110:** C07001, doi:10.1029/2004JC002560

———, A. J. Poulton, D. T. Drapeau, B. C. Bowler, L. A. Windecker, and E. S. Booth. 2011*b*. Zonal and meridional patterns of phytoplankton biomass and carbon fixation in the Equatorial Pacific Ocean, between 110°W and 140°W. Deep-Sea Res. II **58:** 400–416, doi:10.1016/j.dsr2.2010.08.004

———, and P. Utgoff. 2009. Potential interactions among ocean acidification, coccolithophores and the optical properties of seawater. Oceanography **22:** 146–159, doi:10.5670/oceanog.2009.104

Bianchi, A. A., L. Bianucci, A. R. Piola, D. R. Pino, I. Schloss, A. Poisson, and C. F. Balestrini. 2005. Vertical stratification and air-sea CO_2 fluxes in the Patagonian Shelf. J. Geophys. Res. C Oceans **110:** C07003, doi:10.1029/2004JC002488

Boyd, P., J. LaRoche, M. Gall, R. Frew, and R. M. L. McKay. 1999. Role of iron, light, and silicate in controlling algal biomass in subantarctic waters SE of New Zealand. J. Geophys. Res. Oceans **104:** 13395–13408, doi:10.1029/1999JC900009

Boyd, P. W., K. R. Arrigo, R. Strzepek, and G. L. van Dijken. 2012. Mapping phytoplankton iron utilization: Insights into Southern Ocean supply mechanisms. J. Geophys. Res. **117:** C06009, doi:10.1029/2011JC007726

———, R. Strzepek, F. Fu, and D. A. Hutchins. 2010. Environmental control of open-ocean phytoplankton groups: Now and in the future. Limnol. Oceanogr. **55:** 1353–1376, doi:10.4319/lo.2010.55.3.1353

———, and others. 2000. A mesoscale phytoplankton bloom in the polar Southern Ocean stimulated by iron fertilization. Nature **407:** 695–702, doi:10.1038/35037500

Brandini, F. P., D. Boltovskoy, A. R. Piola, A. Kocmur, R. Röttgers, P. C. Abreug, and R. M. Lopes. 2000. Multiannual trends in fronts and distribution of nutrients and chlorophyll in the southwestern Atlantic (30–62°S). Deep-Sea Res. I **47:** 1015–1033, doi:10.1016/S0967-0637(99)00075-8

Bricaud, A., A. Morel, and L. Prieur. 1983. Optical efficiency factors of some phytoplankters. Limnol. Oceanogr. **28:** 816–832, doi:10.4319/lo.1983.28.5.0816

Brown, C. W., and J. A. Yoder. 1994. Coccolithophorid blooms in the global ocean. J. Geophys. Res. **99:** 7467–7482, doi:10.1029/93JC02156

Brzezinski, M., and others. 2011. Co-limitation of diatoms by iron and silicic acid in the equatorial Pacific. Deep-Sea Res. II **58:** 493–511, doi:10.1016/j.dsr2.2010.08.005

Brzezinski, M. A., and D. M. Nelson. 1989. Seasonal changes in the silicon cycle within a Gulf Stream warm-core ring. Deep-Sea Res. I **36:** 1009–1030, doi:10.1016/0198-0149(89)90075-7

de Souza, M. S., C. R. B. Mendes, V. M. T. Garcia, R. Pollery, and V. Brotas. 2012. Phytoplankton community during a coccolithophorid bloom in the Patagonian Shelf: Microscopic and high-performance liquid chromatography pigment analyses. J. Mar. Biol. Assoc. UK **92:** 13–27, doi:10.1017/S0025315411000439

D'Ovidio, F., S. De Monte, S. Alvain, Y. Dandonneau, and M. Lévy. 2010. Fluid dynamical niches of phytoplankton types. Proc. Natl. Acad. Sci. USA **107:** 18366–18370, doi:10.1073/pnas.1004620107

Eppley, R. W., J. N. Rogers, and J. J. McCarthy. 1969. Half-saturation constants for uptake of nitrate and ammonium by marine phytoplankton. Limnol. Oceanogr. **14:** 912–920, doi:10.4319/lo.1969.14.6.0912

Fernández, E., E. Marañón, and W. M. Balch. 1996. Intracellular carbon partitioning in the coccolithophorid *Emiliania huxleyi*. J. Mar. Syst. **9:** 57–66, doi:10.1016/0924-7963(96)00016-4

Ferreira, A., V. M. T. Garcia, and C. A. E. Garcia. 2009. Light absorption by phytoplankton nonalgal particles and dissolved organic matter at the Patagonia Shelf break in spring and summer. Deep-Sea Res. I **56:** 2162–2174, doi:10.1016/j.dsr.2009.08.002

Francois, R., S. Honjo, R. Krishfield, and S. Manganini. 2002. Factors controlling the flux of organic carbon to the bathypelagic zone of the ocean. Global Biogeochem. Cycles **16:** 1087, doi:10.1029/2001GB001722

Gaiero, D. M., J.-L. Probst, P. J. Depetris, S. M. Bidart, and L. Leleyter. 2003. Iron and other transition metals in Patagonian riverborne and windborne materials: Geochemical control and transport to the southern South Atlantic Ocean. Geochim. Cosmochim. Acta **67:** 3603–3623, doi:10.1016/S0016-7037(03)00211-4

Gallegos, C. L., and P. W. Bergstrom. 2005. Effects of a *Prorocentrum* minimum bloom on light availability for and potential impacts on submersed aquatic vegetation in upper Chesapeake Bay. Harmful Algae **4:** 553–574, doi:10.1016/j.hal.2004.08.016

Garcia, C. A. E., and others. 2011. Environmental conditions and bio-optical signature of a coccolithophorid bloom in the Patagonian Shelf. J. Geophys. Res. **116:** 1–17.

Garcia, V. M. T., and others. 2008. Environmental factors controlling the phytoplankton blooms at the Patagonia shelf-break in spring. Deep Sea Res. **55:** 1150–1166, doi:10.1016/j.dsr.2008.04.011

Garzoli, S. L., Z. Garraffo, G. Podesta, and O. Brown. 1992. Analysis of a general circulation model product. 1. Frontal systems in the Brazil/Malvinas and Kuroshio/Oyashio regions. J. Geophys. Res. C Oceans **97:** 20117–20138, doi:10.1029/92JC02222

Haxo, F. T. 1985. Photosynthetic action spectrum of the coccolithophorid, *Emiliania huxleyi* (Haptophyceae): 19′Hexanoyloxyfucoxanthin as antenna pigment. J. Phycol. **21:** 282–287, doi:10.1111/j.0022-3646.1985.00282.x

Hewes, C. D., and O. Holm-Hansen. 1983. A method for recovering nanoplankton from filters for identification with the microscope: The filter-transfer-freeze (FTF) technique. Limnol. Oceanogr. **28:** 389–394, doi:10.4319/lo.1983.28.2.0389

Holligan, P. M., A. Charalampopoulou, and R. Hutson. 2010. Seasonal distributions of the coccolithophore, *Emiliania huxleyi*, and of particulate inorganic carbon in surface waters of the Scotia Sea. J. Mar. Syst. **82:** 195–205, doi:10.1016/j.jmarsys.2010.05.007

———, and others. 1993. A biogeochemical study of the coccolithophore, *Emiliania huxleyi*, in the north Atlantic. Global Biogeochem. Cycles **7:** 879–900, doi:10.1029/93GB01731

Iglesias-Rodriguez, M. D., and others. 2002. Representing key phytoplankton functional groups in ocean carbon cycle models: Coccolithophorids. Global Biogeochem. Cycles **16:** 1–20, doi:10.1029/2001GB001398

Joint Global Ocean Flux Study. 1996. Protocols for the Joint Global Ocean Flux Study (JGOFS) core measurements. *In* A. Knap [ed.], Report No. 19 of the Joint Global Ocean Flux Study. Scientific Committee on Oceanic Research, International Council of Scientific Unions. Intergovernmental Oceanographic Commission.

Leblanc, K., and others. 2009. Distribution of calcifying and silicifying phytoplankton in relation to environmental and biogeochemical parameters during the late stages of the 2005 North East Atlantic spring bloom. Biogeosciences **6:** 2155–2179, doi:10.5194/bg-6-2155-2009

Margalef, R. 1978. Life-forms of phytoplankton as survival alternatives in an unstable environment. Oceanol. Acta **1:** 493–509.

Morel, A., and Y. Ahn. 1991. Optics of heterotrophic nanoflagellates and ciliates: A tentative assessment of their scattering role in oceanic waters compared to those of bacterial and algal cells. J. Mar. Res. **49:** 177–202, doi:10.1357/002224091784968639

Olsson, P., and E. Granéli. 1991. Observations on diurnal vertical migration and phased cell division for three coexisting marine dinoflagellates. J. Plankton Res. **13:** 1313–1324, doi:10.1093/plankt/13.6.1313

Paasche, E., and S. Brubak. 1994. Enhanced calcification in the coccolithophorid *Emiliania huxleyi* (Haptophyceae) under phosphorus limitation. Phycologia **33:** 324–330, doi:10.2216/i0031-8884-33-5-324.1

Painter, S. C., A. J. Poulton, J. T. Allen, R. Pidcock, and W. M. Balch. 2010. The COPAS'08 expedition to the Patagonian Shelf: Physical and environmental conditions during the 2008 coccolithophore bloom. Cont. Shelf Res. **30:** 1907–1923, doi:10.1016/j.csr.2010.08.013

Poulton, A. J., R. Sanders, P. M. Holligan, T. Adey, M. Stinchcombe, L. Brown, and K. Chamberlain. 2006. Phytoplankton mineralisation in the tropical and subtropical Atlantic Ocean. Global Biogeochem. Cycles **20:** GB4002, doi:10.1029/2006GB002712

———, J. R. Young, N. R. Bates, and W. M. Balch. 2011. Biometry of detached *Emiliania huxleyi* coccoliths along the Patagonian Shelf. Mar. Ecol. Prog. Ser. **443:** 1–17, doi:10.3354/meps09445

———, and others. 2013. The 2008 *Emiliania huxleyi* bloom along the Patagonian Shelf: Ecology, biogeochemistry and cellular calcification. Global Biochem. Cycles **27:** 1–11, doi:10.1002/2013GB004641

Poulton, N. J., and J. L. Martin. 2010. Imaging flow cytometry for quantitative phytoplankton analysis—FlowCAM, p. 49–54. *In* B. Karlson, C. Cusack, and E. Bresnan [eds.], Microscopic and molecular methods for quantitative phytoplankton analysis. Vol. 55. Intergovernmental Oceanographic Commission of UNESCO.

Romero, S. I., A. R. Piola, M. Charo, and C. A. E. Garcia. 2006. Chlorophyll-*a* variability off Patagonia based on SeaWiFS data. J. Geophys. Res. **111:** C05021, doi:10.1029/2005JC003244

Satoh, M., K. Iwamoto, I. Suzuki, and Y. Shiraiwa. 2009. Cold stress stimulates intracellular calcification by the coccolithophore, *Emiliania huxleyi* (Haptophyceae) under phosphate-deficient conditions. Mar. Biotechnol. **11:** 327–333, doi:10.1007/s10126-008-9147-0

Siegel, D. A., S. Maritorena, N. B. Nelson, D. A. Hansell, and M. Lorenzi-Kayser. 2002. Global distribution and dynamics of colored dissolved and detrital organic materials. J. Geophys. Res. **107:** 3228, doi:10.1029/2001JC000965

Signorini, S. R., V. M. T. Garcia, A. R. Piola, C. A. E. Garcia, M. M. Mata, and C. McClain. 2006. Seasonal and interannual variability of calcite in the vicinity of the Patagonian Shelf break (38°S–52°S). Geophys. Res. Lett. **33:** L16610, doi:10.1029/2006GL026592

Stæhr, P. A., and J. J. Cullen. 2003. Detection of *Karenia mikimotoi* by spectral absorption signatures. J. Plankton Res. **25:** 1237–1249, doi:10.1093/plankt/fbg083

Townsend, D. W., N. D. Rebuck, M. A. Thomas, L. Karp-Boss, and R. M. Gettings. 2010. A changing nutrient regime in the Gulf of Maine. Cont. Shelf Res. **30:** 820–832, doi:10.1016/j.csr.2010.01.019

Tyrrell, T., and A. H. Taylor. 1995. Latitudinal and seasonal variations in carbon dioxide and oxygen in the northeast Atlantic and the effects on *Emiliania huxleyi* and other phytoplankton. Global Biogeochem. Cycles **9:** 585–604, doi:10.1029/95GB01133

Villareal, T. A. 1988. Positive buoyancy in the oceanic diatom *Rhizosolenia debyana* H. Peragallo. Deep-Sea Res. **35:** 1037–1045.

Voss, K., W. M. Balch, and K. A. Kilpatrick. 1998. Scattering and attenuation properties of *Emiliania huxleyi* cells and their detached coccoliths. Limnol. Oceanogr. **43:** 870–876, doi:10.4319/lo.1998.43.5.0870

Winter, A., J. Henderiks, L. Beaufort, R. E. M. Rickaby, and C. W. Brown. 2014. Poleward expansion of the coccolithophore *Emiliania huxleyi*. J. Plankton Res. **36:** 316–325, doi:10.1093/plankt/fbt110

Yoder, J. A., S. G. Ackleson, R. T. Barber, P. Flament, and W. M. Balch. 1994. A line in the sea. Nature **371:** 689–692, doi:10.1038/371689a0

Zondervan, I. 2007. The effects of light, macronutrients, trace metals and CO_2 on the production of calcium carbonate and organic carbon in coccolithophores—a review. Deep-Sea Res. II **54:** 521–537, doi:10.1016/j.dsr2.2006.12.004

Associate editor: Dariusz Stramski

Received: 04 September 2013
Accepted: 01 April 2014
Amended: 29 May 2014